Chapter
Microassembly

Karl F. Böhringer, Ronald S. Fearing, Ken Y. Goldberg, University of California, Berkeley

1 Introduction

The trend toward miniaturization of mass-produced products such as disk drives, wireless communication devices, displays, and sensors will motivate fundamental innovation in design and production; microscopic parts cannot be fabricated or assembled in traditional ways. Some of the parts will be fabricated using processes similar to VLSI technology, which allows fast and inexpensive fabrication of thousands of components in parallel. Whereas a primary challenge in industrial robotics is how to securely grasp parts, at the micro scale, where electrostatic and van der Waals adhesion forces dominate, the challenge is: how to release parts?

Microassembly lies between conventional (macro-scale) assembly (with part dimensions $> 1\,mm$) and the emerging field of nanoassembly (with part dimensions in the molecular scale, *i.e.*, $< 1\,\mu m$). Currently, microassembly is performed largely by humans with tweezers and microscopes or with high precision pick-and-place robots. Both methods are inherently serial. Since individual parts are fabricated in parallel, it is intriguing to consider how they might be *assembled* in parallel (see Figure 1).

Microassembly poses new challenges and problems in design and control of hardware and software tools. These problems are discussed in the following section, which investigates the effects of down-scaling on parts handling, and gives a survey of sticking effects. Section 3 introduces a taxonomy of microassembly. In Section 4 we give an overview of recent work on microassembly. Section 5 describes a new approach towards massively-parallel, stochastic micro assembly. We conclude this chapter with an outlook on open problems and future trends.

Automated microassembly poses a list of new challenges to the robotics community. Conventional high-accuracy robots have a control error of $100\,\mu m$ at best, which would translate to relative errors of 100% or more. Obtaining accurate sensor data is equally difficult. Sensors cannot be easily placed on tiny precision instruments without making them bulky or compromising their functionality. Image processing is one alternative, but it is still slow, costly, difficult to program, and susceptible to reflection and other noise. Moreover, the view may be obstructed by tools that are orders of magnitude larger than the parts being handled. Even when reliable images are obtained, one major challenge is how to coordinate and calibrate gross actuator motion with sensor data.

Models based on classical mechanics and geometry have been used to describe microassembly processes. However, due to scaling effects, forces that are insignificant at the macro scale become dominant at the micro scale [24, 67]. For example, when parts to be
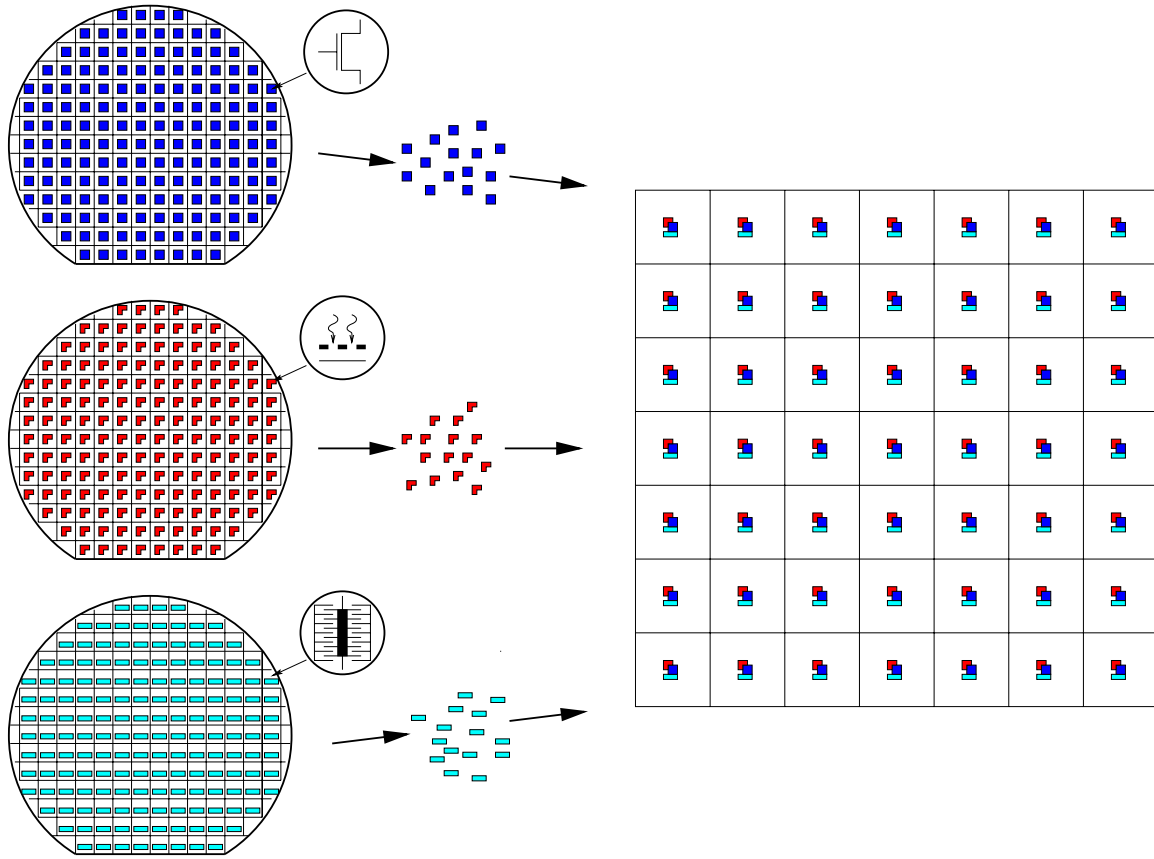
Figure 1: Parallel microassembly: Multiple micro-scale components (e.g. electronics, photonics, and MEMS) are built in parallel using standard manufacturing processes. They are positioned and combined with other components on a hybrid "pallet." Note that the fabrication density is very high, while the pallets may have a larger size and lower density. (Reprinted from [12]. © 1998 IEEE.)

handled are less than one millimeter in size, adhesive forces between gripper and object can be significant compared to gravitational forces. These adhesive forces arise primarily from surface tension, van der Waals, and electrostatic attractions and can be a fundamental limitation to part handling. While it is possible to fabricate miniature versions of conventional robot grippers, for example from polysilicon (see Figure 2 [39], or [57]) overcoming adhesion effects for the smallest parts will be difficult. Thus, manipulation of parts on the order of 10 micron or smaller may best be done in a fluid medium using techniques such as laser trapping, or dielectrophoresis.

Interest in microassembly has been fueled by the availability of new components made of integrated circuits (ICs) and micro electro mechanical systems (MEMS). The exponential increase in computing power of ICs has been made possible to a large extent by the dramatic advances in process miniaturization and integration. MEMS technology directly taps into this highly developed, sophisticated technology. MEMS and IC share the efficient, highly
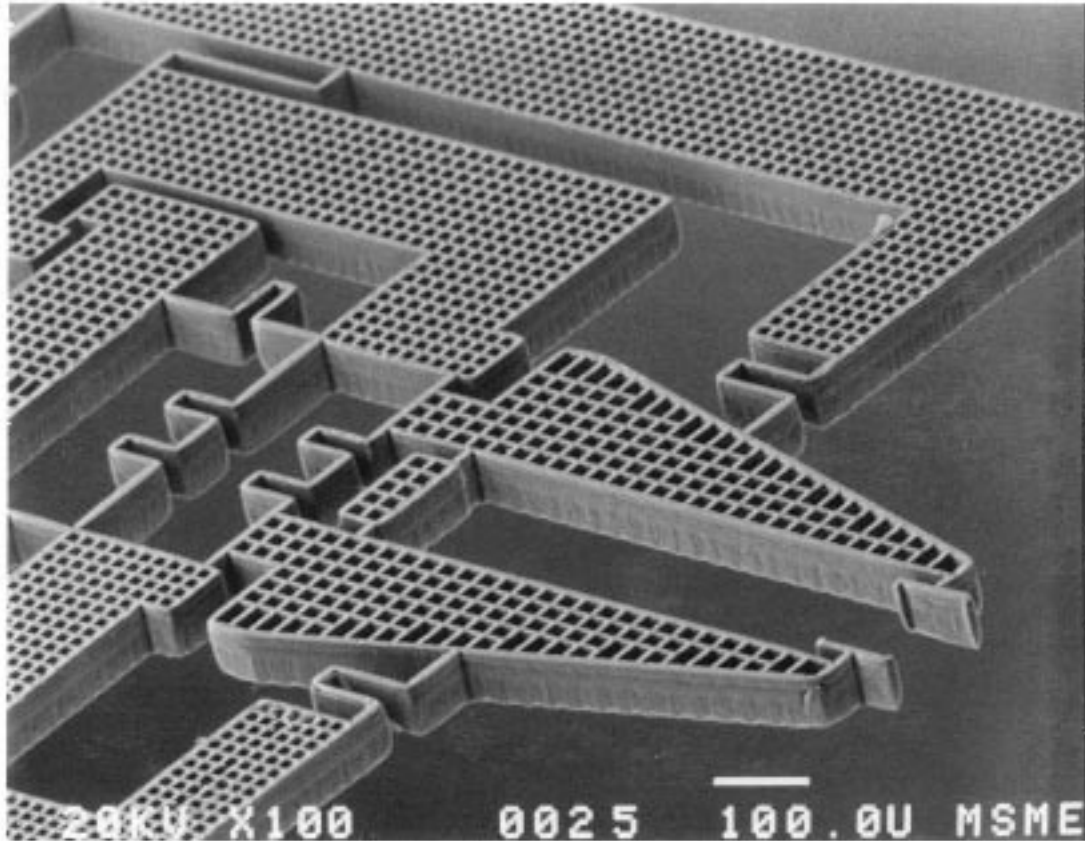
Figure 2: Microgripper made of high aspect ratio molded polycrystalline silicon. The white bar at the bottom of the picture represents $100\,\mu m$. The actuator is an electrically heated thermal expansion beam which causes the compound lever linkage to move the tips. (SEM photograph courtesy of Chris Keller, Berkeley Sensor and Actuator Center.)

automated fabrication processes using computer aided design and analysis tools, lithographic pattern generation, and micromachining techniques such as thin film deposition and highly selective etching. Unlike ICs, MEMS include *mechanical* components, whose sizes typically range from about ten μm to a few hundred μm, with smallest feature sizes of less than a micron and overall sizes of up to a millimeter or more. While recent years have brought an explosive growth in new MEMS devices ranging from accelerometers, oscillators, micro optical components, to micro-fluidic and biomedical devices, interest is now shifting towards complex microsystems that combine sensors, actuators, computation, and communication in a single micro device [6]. It is widely expected that these devices will lead to dramatic developments and a flurry of new consumer products, in analogy to the microelectronics revolution.

Current micro systems generally use *monolithic* designs in which all components are fabricated in one (lengthy) sequential process. In contrast to the more standardized IC manufacture, a feature of this manufacturing technology is the wide variety of non-standard processes and materials that may be incompatible with each other. These incompatibilities
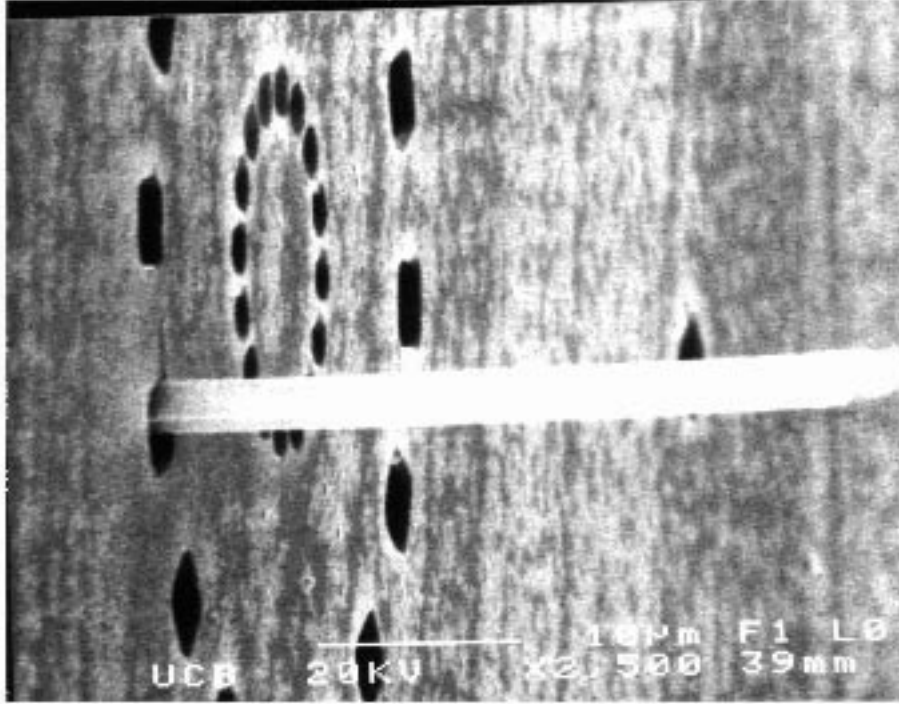
3

Figure 3: The peg-in-hole problem at micro-scale. A $1 \times 4 \times 40\,\mu m$ silicon oxide peg was inserted into a $4 \times 4 \times 12\,\mu m$ square hole by using a microgripper as shown in Figure 2. (SEM photograph courtesy of Chris Keller, Berkeley Sensor and Actuator Center.)

severely limit the manufacture of more complex devices. A possible solution to these problems is *microassembly*, which is the discipline of positioning, orienting, and assembling of micron-scale components into complex micro systems.

The goal of microassembly is to provide a means to achieve *hybrid* micro-scale devices of high complexity, while maintaining high yield and low cost: various IC and MEMS components are fabricated and tested individually before being assembled into complete micro systems.

2 Sticking Effects for Micro Parts Handling

A typical robotic manipulation scenario is the sequence of operations pick, transport, and place. For parts with masses of several grams, the gravitational force will usually dominate adhesive forces, and parts will drop when the gripper opens. For parts with size less than a millimeter (masses less than $10^{-6}kg$), the gravitational and inertial forces may become insignificant compared to adhesive forces, which are generally proportional to surface area. When parts become very small, adhesive forces can prevent release of the part from the gripper. For example, a laser diode for an optical disk may be only $300\,\mu m$ in size [28]. Figure 4 illustrates some of the effects which can be seen when attempting to manipulate micro parts. As the gripper approaches the part, electrostatic attraction may cause the part
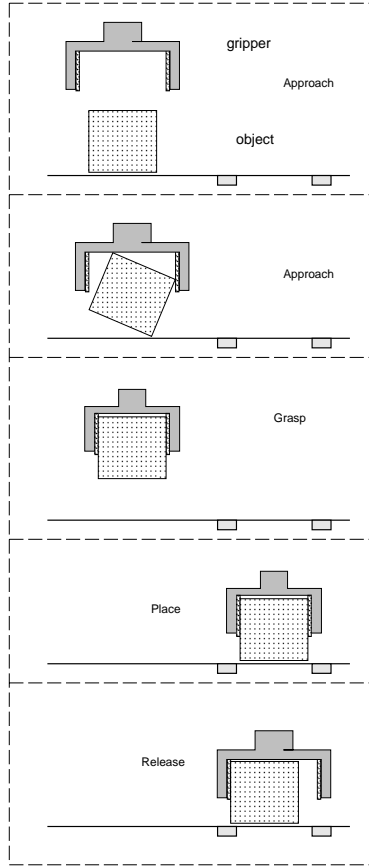
Figure 4: Pick-move-place operation with micro-parts. Due to sticking effects, parts may be attracted to the gripper during the approach and release phase, causing inaccurate placement. (Reprinted from [24]. © 1995 IEEE.)

to jump off the surface into the gripper, with an orientation dependent on initial charge distributions. When the part is placed to a desired location, it may adhere better to the gripper than the substrate, preventing accurate placement.

Adhesion could be due to electrostatic forces, van der Waals forces, or surface tension. Electrostatic forces arise from charge generation (triboelectrification) or charge transfer during contact. Van der Waals forces are due to instantaneous polarization of atoms and molecules due to quantum mechanical effects [34]. Surface tension effects arise from interactions of layers of adsorbed moisture on the two surfaces. The goal of this section is to survey causes of adhesion, provide estimates on the magnitude of their effect, and to survey methods for reducing the effect of adhesive forces.

For a simple numerical example to get an idea of the scale of the adhesion forces, consider the force between a spherical object and a plane (such as one finger of the gripper in Figure 5). The approximate force between a charged sphere and a conducting plane is given by:

$$F_{elec} = \frac{q^2}{4\pi\epsilon(2r)^2} , \tag{1}$$

where q is charge, ϵ is the permittivity of the dielectric, and r is object radius. The assumed
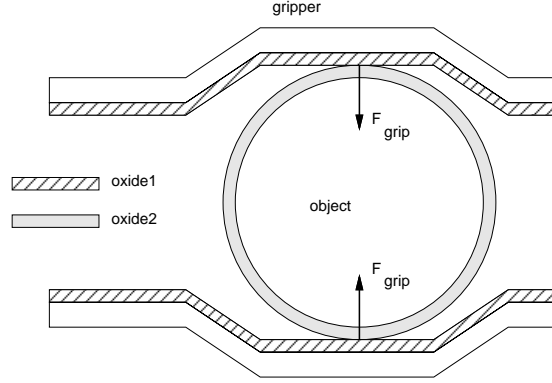
5

Figure 5: Micro-gripper holding spherical object. (Reprinted from [24]. © 1995 IEEE.)

charge density is approximately $1.6 \times 10^{-6} Cm^{-2}$. It is interesting to note that the contact of good insulators such as smooth silica and mica can result in charge density up to $10^{-2} Cm^{-2}$ with pressures on the order of $10^6 Pa$ at $1 \, \mu m$ distance [32].

The van der Waals force for a sphere and plane is given approximately by [14] as:

$$F_{vdw} \;\; = \;\; \frac{hr}{8\pi z^2}, \tag{2}$$

where h is the Lifshitz-van der Waals constant, and z is the atomic separation between the surfaces. Of course, this formula is assuming atomically smooth surfaces; severe corrections need to be made for rough surfaces as the van der Waals forces fall off very rapidly with distance. For a rough estimate, we will assume a true area of contact of 1% of apparent area, or estimated force 1% of maximum predicted with smooth surfaces.

In a high humidity environment, or with hydrophilic surfaces, there may be a liquid film between the spherical object and planar surface contributing a large capillary force [1]:

$$F_{tens} \;\; = \;\; \frac{\gamma(cos\theta_1 + cos\theta_2)A}{d}, \tag{3}$$

where γ is the surface tension ($73 \, mNm^{-1}$ for water), A is the shared area, d is the gap between surfaces, and θ_1, θ_2 are the contact angles between the liquid and the surfaces. Assuming hydrophilic surfaces and a separation distance much smaller than the object radius [14, 73]:

$$F_{tens} \;\; = \;\; 4\pi r\gamma, \tag{4}$$

where r is the object radius.

For a spherical part of silicon the gravitational force is:

$$F_{grav} \;\; = \;\; \frac{4}{3}\pi r^3 \rho_{Si} g, \tag{5}$$

where $\rho_{Si} \;\; = \;\; 2300 \, kgm^{-3}$ is the density of silicon. Figure 6 shows the comparison of forces. For accurate placement, adhesion forces should be an order of magnitude less than gravitational forces. Capillary forces dominate and must be prevented to allow accurate
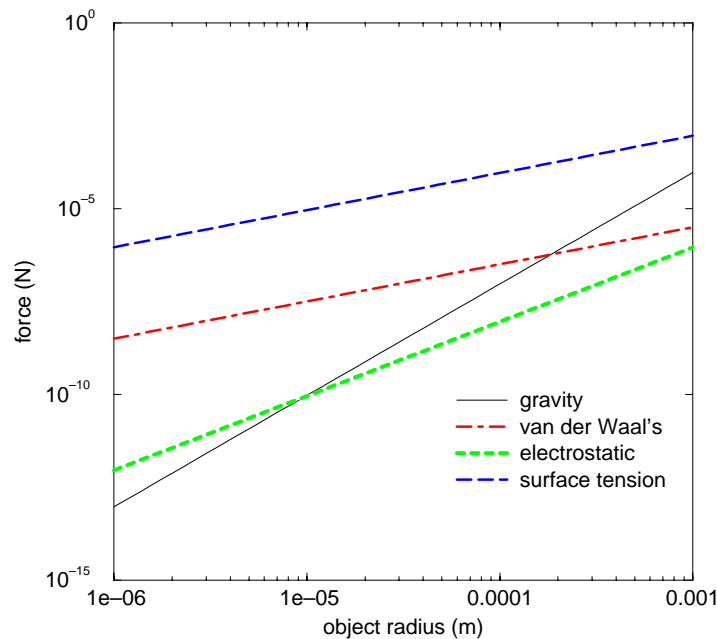
Figure 6: Gravitational, electric, van der Waals, and surface tension forces. Attractive force between sphere and plane. (Reprinted from [24]. © 1995 IEEE.)

placement. Van der Waals forces can start to be significant (with smooth surfaces) at about $100\,\mu m$ radius, and generated electric charges from contacts could prevent dry manipulation of parts less than $10\,\mu m$ in size.

While Figure 6 shows electrostatic to be the least significant force except for gravity, it can be argued that it is actually the most significant force for grasping and manipulation of $10\,\mu m$ to $1\,mm$ parts. First, the van der Waals force is only significant for gaps less than about $100\,nm$ [65, 34]. Unless rigid objects are very smooth, the effective distance between the object and the gripper will be large except at a few points of contact. Second, actual contact with a fluid layer needs to be made for surface tension to be significant, and a dry or vacuum environment could be used to eliminate surface tension effects. Finally, the electrostatic forces can be active over ranges of the order of the object radius. Surface roughness is much less important for electrostatic forces than for van der Waals.

2.1 Literature on Adhesion

The adhesion of particles to substrates has received substantial study for problems such as particulate contamination in semiconductor manufacturing [43, 79, 14, 30, 35]. The recent developments in micro electro mechanical systems (MEMS), disk drives, and microassembly have stimulated the study of friction effects at the micro-scale. The normal Coulomb friction effects seen at the macro-scale are quite different at the micro-scale, with large adhesive components. Several studies have examined surfaces using the atomic force microscope [73,

36]. A common problem in MEMS devices is that free standing micro-structures tend to stick to the substrate after being released during processing. The dominant mechanisms for sticking in these devices (which are typically constructed as a cantilever plate suspended 1 or 2 μm above the substrate) appears to be surface tension pulling the plate down, followed by van der Waals bonding. Recent papers have studied this problem [4] and proposed solution methods of making the surfaces rough and hydrophobic [45, 1, 2, 65].

2.2 Adhesion Due to Electrostatic Forces

Ensuring that parts and grippers are electrically neutral is difficult [29]. Significant amounts of charge may be generated by friction forces and differences in contact potentials. While grounded conductors will drain off charge, insulators can maintain very high surface charge distributions. The local field intensity near a surface charge distribution can be estimated using Gauss's Law and Figure 7. Neglecting any interior field, the boundary conditions give

$$\hat{z} \cdot \epsilon_o \vec{E}(z = 0) \; = \; \sigma_s, \tag{6}$$

where $\vec{E}$ is the electric field, $\hat{z}$ is the surface normal, and σ_s is the surface charge density Cm^{-2}. The near field approximation for a surface charge is then:

$$\vec{E} \approx \frac{\sigma_s}{\epsilon_o}\hat{z} \; . \tag{7}$$

The force per unit area for parallel plates is

$$P \; = \; \frac{1}{2}\epsilon_o|E|^2 \; = \; \frac{\sigma_s^2}{2\epsilon_o} \; , \tag{8}$$

where P is the pressure in Pascals.

   At atmospheric pressure and centimeter size gaps, the breakdown strength of air (about $3 \times 10^6 \, Vm^{-1}$ [49]) limits the maximum charge density to about $3 \times 10^{-5} \, Cm^{-2}$, or peak pressures of about $50 \, Pa$. Let l be the length of a side of a cube of silicon. Then the smallest cube which will not stick due to electrostatic force is:

$$l \; = \; \frac{\sigma_s^2}{2\epsilon_o \rho_{Si} g} \; , \tag{9}$$

or about $2 \, mm$ minimum size. Of course, a uniform charge distribution over such a large area is unlikely, although there could be local concentrations of charge of such magnitude. However, at very small gaps of the order of $1 \, \mu m$ (less than the mean free path of an electron in air), fields two orders of magnitude higher have been observed [32].

2.2.1 Contact Electrification

When two materials with different contact potentials are brought in contact, charge flows between them to equalize this potential. For metal-metal contact [49, 43], a rough approximation to the surface charge density is:

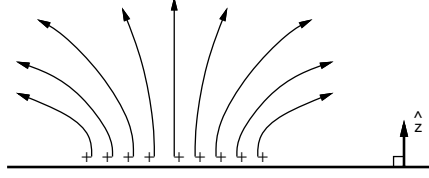$$\sigma_s \; = \; \frac{\epsilon_o U}{z_o} \tag{10}$$

8

Figure 7: Field approximation near surface charge distribution. (Reprinted from [24]. © 1995 IEEE.)

Materials in contact	charge density mCm^{-2}	electrostatic pressure Nm^{-2}	condition	ref.
SiO$_2$ - Al	2.0	2×10^5	1mPa N$_2$ 80nm SiO$_2$	Lowell '90 [48]
soda glass - Al	0.13	10^3		
SiO$_2$ - mica	5–20	1.4×10^6 to 20×10^6	N$_2$ at STP "atomically smooth"	Horn & Smith 92 [32]
epoxy - Cu	0.04	100	$10^4 Pa$ air	Kwetkus et al. 91 [44]
glass - Au	4.2	10^6	air	Harper '67 [29]
nylon - steel	.0036	1	40 − 60% RH	
polystyrene	.0002	2×10^{-6}		

Table 1: Charge from contact electrification. Pressure is the effective pressure due to the generated charge. (Reprinted from [24]. © 1995 IEEE.)

where U is the contact potential difference, which is typically less than 0.5 V, and z_o is the gap for tunneling, about 1nm. Consider two metal spheres (insulated from their surroundings) brought into contact, then slowly separated. With a contact potential of 0.5 V, the initial charge density according to eq.(10) will be about $4\,mCm^{-2}$, with field strength $5 \times 10^8\,Vm^{-1}$. For small gaps (order 1nm), electron tunneling and field emission [49] will transfer charge, and then for larger gaps (order $1\,\mu m$) air breakdown can occur. In laboratory experiments, contact electrification has been shown to generate significant charge density, which could cause adhesion (see Table 1).

2.2.2 Charge Storage in Dielectrics

In principle, using conductive grippers can reduce static charging effects. However, the objects to be handled, such as silicon parts, can be covered with good insulator layers, such as native oxides. Up to $1\,nm$ of native oxide is possible after several days in air at room temperature [53]. This native oxide is a very good insulator, and can withstand a maximum field strength of up to $3 \times 10^9\,Vm^{-1}$ [72]. This implies that significant amounts of charge can be stored in the oxide. With the permittivity of silicon $\epsilon = 3.9\epsilon_o$, peak pressures according to eq. (8) are on the order of $10^8 Pa$. With a contact area of only $10(nm)^2$, this would be a force of $10\,nN$, enough to support a $30\,\mu m$ cube against gravity.

Consider an initially charged object grasped as shown in Figure 5, by a grounded gripper. In regions where the two dielectrics are not in contact, charge will be induced on the opposite surface. As suggested in Figure 8, local regions of charge can remain in the dielectric layer
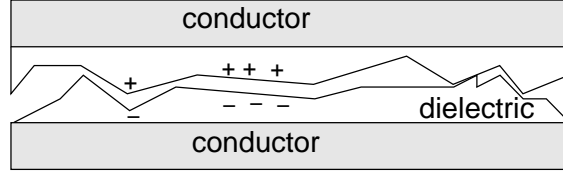
9

Figure 8: Physical model of contact with charge in oxide layer. (Reprinted from [24]. © 1995 IEEE.)
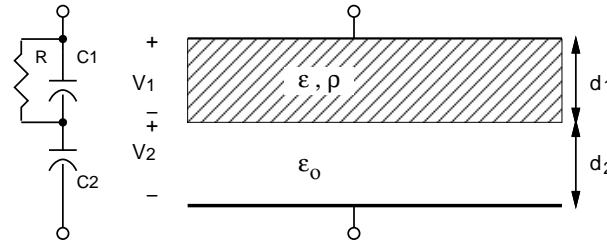

Figure 9: Equivalent circuit model of contact. ρ is the resisitivity of the dielectric. (Reprinted from [24]. © 1995 IEEE.)

in spite of "intimate" contact between two nominal conductors. The surface roughness can prevent charge neutralization through intimate contact of oppositely charged regions. The residual charge can cause adhesion.

It can be very difficult to remove stored charge in a dielectric layer. Consider a simplistic model for the electrical contact, with one capacitor representing the air gap and a second capacitor in series representing the dielectric layer as shown in Figure 9. It is apparent that shorting the terminals will not instantaneously remove charge from both capacitors, hence there will be a residual attraction force between the gripper and the object. The stored charge (and hence electric field) decays as a first order exponential, with time constant:

$$\tau = \rho(\epsilon + \epsilon_o \frac{d_1}{d_2}) \tag{11}$$

where ρ is the resistivity of the dielectric. For SiO_2 with resistivity $\rho = 10^{12} \Omega m$, dielectric thickness 10 nm, and air gap 20 nm, the time constant τ is about 40 seconds, significantly reducing cycle time. Charge storage in dielectric layers may result in undesired adhesions in electrostatic grippers [54] and in electrostatic micro-actuators where contact is made with an insulating layer[3].

2.3   Summary

As we have seen, electrostatic, van der Waals, and surface tension forces can be significant compared to the weight of small parts. Conventional assembly methods such as pick-move-place do not scale well for sub-millimeter parts. One possible attractive alternative is assembly while immersed in a fluid, which eliminates electrostatic and surface tension effects [75].

There are several design strategies which can be used to reduce adhesive effects in micro-grippers. Figure 10 compares finger tip shapes. Clearly, the spherical fingertip has reduced

Grasping with Spherical Fingertips

Side view

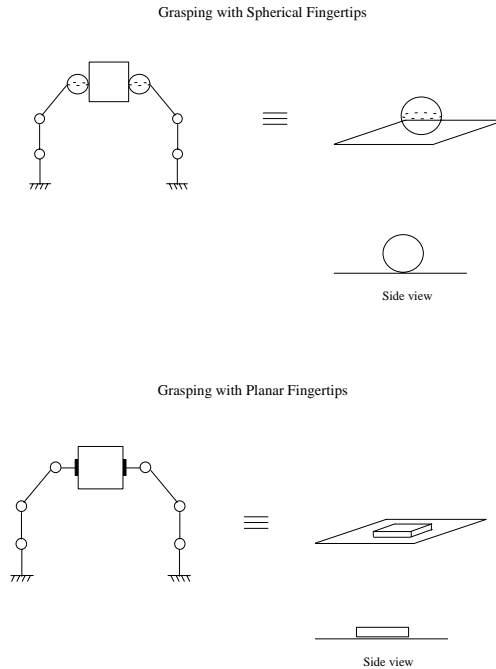Grasping with Planar Fingertips

Side view

Figure 10: Comparison of finger types for grasping. A spherical fingertip will minimize electrostatic and surface tension forces, and can be roughened to minimize van der Waals forces. (Reprinted from [24]. © 1995 IEEE.)

surface contact area and better adhesive properties, unlike polysilicon micro-grippers fabricated using planar surface micro-machining.

Proper choice of gripper materials and geometry can be used to reduce adhesion:

1. Minimize contact electrification by using materials with a small contact potential difference for the gripper and object.
2. Use conductive materials which don't easily form highly insulating native oxides.
3. Gripper surfaces should be rough to minimize contact area.
4. The high contact pressure from van der Waals and electrostatic forces can cause local deformation at the contact site [14]. This deformation can increase the contact area and increase the net adhesive force. Hard materials are preferable to rubber or plastic.
5. A dry atmosphere can help to reduce surface tension effects. Surface tension can be used to help parts adhere better to the target location than the gripper.
6. Free charges such as in ionized air can combine with and neutralize exposed surface charges.

As discrete parts are designed continually smaller to make equipment smaller, more economical and higher performance, there will be a greater need for understanding how to manipulate and assemble micro-parts. Because of adhesive forces, grasping and particularly ungrasping of these parts can be complicated. Good models of surfaces and the physics of contact will be needed to implement reliable manipulation and assembly systems.

3   Techniques for Microassembly

Current micromachined devices generally use *monolithic* designs in which all components are fabricated in one (lengthy) sequential process. Recently, microassembly has been proposed as a means to achieve *hybrid* micro-scale devices of high complexity, while maintaining high yield and low cost: various electronic and mechanical components are fabricated and tested individually before being assembled into complete systems (see e.g. [19, 15, 33, 76, 77, 55, 9]).

   In this section we attempt to characterize the techniques currently in use for microassembly. Since microassembly is a new and very active area of research, this characterization may not be complete, and other taxonomies are certainly possible.

3.1   A Taxonomy of Microassembly

1. Serial microassembly: parts are put together one-by-one according to the traditional pick-and-place paradigm. Serial microassembly includes the following techniques:

   - Manual assembly with tweezers and microscopes.

   - Visually based and teleoperated microassembly [55, 25].

   - High precision macroscopic robots: stepping motors and inertial drives are used for sub-micrometer motion resolution (see *e.g.* [59, 78, 21], or MRSI[1] assembly robots for surface-mount electronics components of sub-millimeter size).

   - Micro-grippers ([41, 57, 38, 39], see *e.g.* Figure 2) with gripper sizes of $100\,\mu m$ or less.

2. Parallel microassembly: multiple parts (of identical or different design) are assembled simultaneously. We distinguish two main categories:

   - Deterministic: The relationship between part and its destination is known in advance.
      - Flip-chip wafer-to-wafer transfer: a wafer with partially released components is carefully aligned and pressed against another substrate. When the wafers are separated again, the components remain bonded to the second substrate ([17, 68], see *e.g.* Figure 11).
      - Micro gripper arrays [39] capable of massively-parallel pick-and-place operations.
   - Stochastic: The relationship between the part and its destination is unknown or random. The parts "self-assemble" during stochastic processes in analogy to annealing. The following effects can be used as motive forces for stochastic self-assembly.
      - Fluidic agitation and mating part shapes [76, 77, 75].
      - Vibratory agitation and electrostatic force fields [15, 18, 9, 12].
      - Vibratory agitation and mating part shapes [33].
      - Mating patterns of self-assembling monolayers [69].

---

[1]MRSI International, 25 Industrial Ave., Chelmsford, MA 01824.

3.2 A Hierarchy of Assembly Forces

We already noted in the introduction that for parts of dimensions $1\,mm$ or less, surface adhesion forces may dominate "volume" forces such as gravity or inertia. Parts are trapped in locations where these adhesion forces are sufficiently strong, and may not be released (for example from a micro gripper) even if traditional (macroscopic) dynamical analysis does not show force closure. Hence it is essential to have control over these forces during microassembly. One common technique to overcome adhesion is to employ vibration. Note however that since this technique relies on the inertia of the parts, vibration becomes less efficient with decreasing part sizes, *i.e.*, higher vibration amplitudes or frequencies are necessary for smaller parts.

As an example, consider the task of palletizing micro parts (as described in Figure 1 or Section 5). During the assembly process, adhesion forces have to be overcome in the initial positioning phase as well as the final bonding phase. However, adhesion is used to keep the parts in place during the part transfer phase.

1. Positioning: forces provided by vibration are larger than trapping forces (van der Waals, electrostatic, surface tension). The part can move freely and exhibits trajectories resembling Brownian motion.

2. Annealing: the vibration forces are gradually reduced until the trapping forces dominate. The part settles at a local potential minimum.

3. Bonding: target spot adhesion (*e.g.* by indium soldering during wafer-to-wafer transfer) is greater than the trapping forces. Permanent bonds are created between part and target substrate.

3.3 Issues and Problems

Earlier work on microfabrication has looked almost exclusively at *in-situ* batch fabrication, where (in accordance with the IC fabrication paradigm) all components are built in one fabrication process on a substrate (usually a silicon wafer). The shortcomings of this approach have already been outlined in the Introduction. They include

Incompatible Materials: for example, many opto-electronics require GaAs substrates which are incompatible with standard electronics.

Incompatible Processes: for example, processes requiring high temperatures destroy CMOS circuitry.

Exponential Decline in Yield: each step in a processing sequence has a non-zero failure probability associated with it. These probabilities multiply and hence dramatically reduce the yield for long processing sequences, prohibiting a complex process generated by simple concatenation of standard processes.

Microassembly overcomes these problems and makes possible *hybrid* devices with otherwise incompatible materials such as e.g. bipolar transistors, MOSFETs, photoelectronic components, and mechanical structures.

4 Recent Research in Microassembly

Vibration has been widely in use in industrial parts feeders. A parts feeder is a machine that singulates, positions, and orients bulk parts before they are transferred to an assembly station. The most common type of parts feeder is the *vibratory bowl feeder*, where parts in a bowl are vibrated using a rotary motion, so that they climb a helical track. As they climb, a sequence of baffles and cutouts in the track create a mechanical "filter" that causes parts in all but one orientation to fall back into the bowl for another attempt at running the gauntlet [13, 62, 64]. Sony's APOS parts feeder [31] is another example of using vibration for parts handling. It uses an array of nests (silhouette traps) cut into a vibrating plate. The nests and the vibratory motion are designed so that the part will remain in the nest only in one particular orientation. By tilting the plate and letting parts flow across it, the nests eventually fill up with parts in the desired orientation. Although the vibratory motion is under software control, specialized mechanical nests must be designed for each part [52].

The term "self-assembly" has been applied to spontaneous ordering processes such as crystal and polymer growth. Recently it has been proposed for the manufacture of systems incorporating large numbers of micro-devices. Positioning, orienting, and assembly is done open-loop, without sensor feedback. The principle underlying the APOS system (controlled vibration to provide stochastic motion, combined with gravity as a motive force for parallel, non-prehensile manipulation) is well-suited for micro-self-assembly. Stochastic microassembly often encompasses vibration in combination with electrostatic, fluidic, and other forces which operate on singulated parts in various media (fluids, air, or vacuum).

In 1991, Cohn, Kim, and Pisano reported on stochastic assembly experiments that use vibration and gravitational forces to assemble periodic lattices of up to 1000 silicon chiplets [19]. Following work demonstrated the use of patterned electrodes to enable assembly of parts in arbitrary 2D patterns. In addition, hydrophobic-hydrophilic interactions in liquid media were employed for 3D self-assembly of millimeter-scale parts [15]. Electrostatic levitation traps were also described by Cohn, Howe, and Pisano, with the aim of controlling friction [18]. This work demonstrated a novel type of electrostatic interaction essentially unique to the micromechanical regime. Recent results by Böhringer, Goldberg, and the above authors have demonstrated the ability to break surface forces using ultra-low amplitude vibration in vacuum ambient [9]. This promises an extremely sensitive technique for positioning parts, as well as discriminating part orientation, shape, and other physical properties.

Smith et al. have demonstrated high-yield assembly of up to 10,000 parts using fluidic self-assembly [76, 77]. Work to date has focused on fabrication of parts and binding sites with desired trapezoidal profiles, surface treatments for control of surface forces, as well as mechanical and electrical interconnection of assembled parts. Parts have included both silicon and III-V devices. Semiconductor junction lasers were suspended in liquid and trapped in micromachined wells on a wafer by solvent-surface forces.

Hosokawa et al. have analyzed the kinetics and dynamics of self-assembling systems by employing models similar to those used to describe chemical reactions. They performed assembly experiments with planar parts of various simple geometries at macro and micro scales (for example, assemblies of hexagons from isoscele triangles) [33].

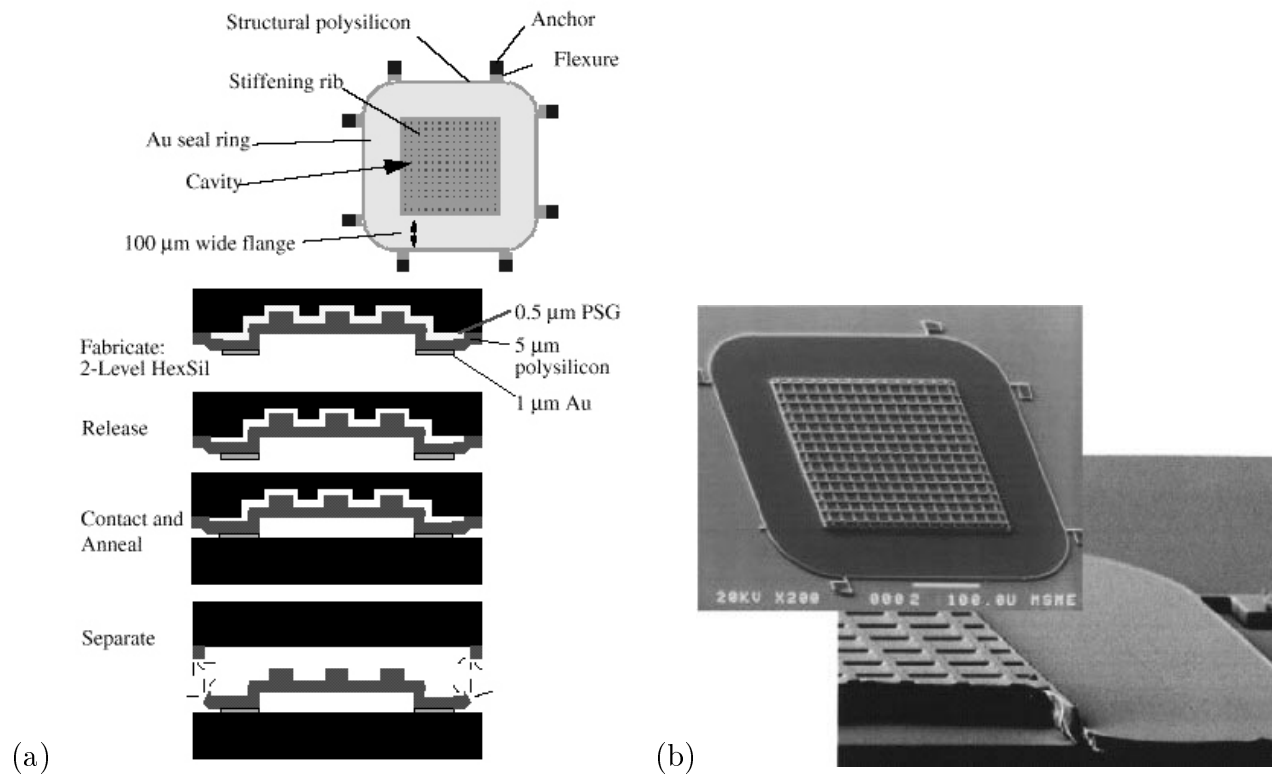Deterministic parallel assembly techniques have been developed by Cohn and Howe for

(a)

(b)

Figure 11: Microassembly by wafer-to-wafer transfer using breakaway tethers. (a) Process flow for a wafer-to-wafer transfer task. (b) Above: a micro shell structure after wafer-to-wafer transfer. Below: cleaved cross-section of the micro shell. (Images courtesy of Michael Cohn [16], Berkeley Sensor and Actuator Center).

wafer-to-wafer transfer of MEMS and other microstructures [20, 17]. In their flip-chip process, the finished microstructures are suspended on break-away tethers on their substrate (Figure 11). The target wafer with Indium solder bumps is precisely aligned and pressed against the substrate, such that the microstructures are cold-welded onto the target wafer. This technique is well-suited for fragile parts. However, it is not appropriate for large numbers of small parts, since the tether suspensions and solder bumps require too much surface area. High-quality electrical, mechanical, and hermetic bonds have been demonstrated by Singh et al. [68]. Parts of $10 - 4000\mu m$ size have been transferred, including functioning microresonators and actuators. High yield ($> 99\%$) as well as $0.1\mu m$ precision have been demonstrated.

By downscaling and parallelizing the concept of a robot gripper, Keller and Howe have demonstrated micro grippers ([38, 39], Figure 2) and propose gripper arrays for parallel transfer of palletized micro parts. Arai and Fukuda (Nagoya) built a manipulator array with heated micro holes [5]. When the holes cool down, they act as suction cups whose lower pressure holds appropriately shaped objects in place. Heating of the cavities increases the pressure and causes the objects to detach from the manipulator.

Quaid and Hollis built extremely accurate systems for precision robotic assembly [59]. Vikramaditya and Nelson used teleoperation and visual feedback for microassembly [55],

Several groups of MEMS researchers have designed and built actuator arrays for micromanipulation, which usually consist of a regular grid of "motion pixels." Devices were built, among others, by Pister et al. [56], Fujita et al. [26], Böhringer et al. [11], Kovacs et al. [70, 71], and Will et al. [46, 47].

MEMS actuator arrays that implement *planar force fields* were proposed by Böhringer et al. who also built single-crystal silicon actuator arrays for micromanipulation tasks [11]. Micro cilia arrays fabricated by Suh et al. [71] were extensively used in their experiments, which successfully demonstrated strategies for parts translating, orienting, and centering [10]. This research in micromanipulation, which built on recent advances in sensorless manipulation (see Erdmann and Mason [22], and Goldberg [27]), again motivated various new macroscopic devices such as vibrating plates (see Böhringer et al. [8, 7], and Reznik et al. [61]) or a "virtual vehicle" consisting of a two-dimensional array of roller wheels that can generate motion fields in the plane (see [50, 51]). We expect this cross-fertilization between macro and micro robotic systems to continue and expand in the future.

Research in MEMS and microassembly is substantially different from the rapidly growing research in nanotechnology, which endeavors to design and construct materials and devices at a molecular scale. Components typically consist of individual molecules or atoms, with dimensions in the nanometer range ($1nm = 10^{-9}m$) — approximately three to four orders of magnitude below the range of microassembly. This chapter focuses solely on microtechnology. Microtechnology is generally seen as "top-down" discipline whose goal is to scale down traditional mechanisms. It draws from classical mechanics, robotics, and control theory. In contrast, nanotechnology constitutes a "bottom-up" approach from individual atoms and molecules to nanomachines. Its science base includes molecular chemistry and physics. Nevertheless, chemistry also serves as an inspiration and paradigm for microassembly, and models of chemical reactions can be used to analyze stochastic assembly of microcomponents (see Section 5). Recent groundbreaking work in nanoassembly has been performed by

Whitesides et al. [66, 58, 74].

5 Stochastic Microassembly with Electrostatic Force Fields

Currently, microassembly is performed by humans with tweezers and microscopes or with high precision pick-and-place robots. Both methods are inherently serial. Since individual parts are fabricated in parallel, it is intriguing to consider how they might be *assembled* in parallel. In this section we propose a concept for massively parallel assembly.

The idea is to arrange microscopic parts on a reusable pallet and then to press two pallets together, thereby assembling the entire array in parallel. We focus on how to position and align an initially random collection of identical parts. This approach builds on the planning philosophy of sensorless, nonprehensile manipulation pioneered by Erdmann and Mason [22]. To model electrostatic forces acting on parts moving on a planar surface, we use the *planar force field*, an abstraction defined with piecewise continuous functions on the plane that can be locally integrated to model the motion of parts [11].

Planar force fields, as defined by the magnitude and direction of force at each point, can be designed to position, align and sort arrays of microscopic parts in parallel. Developing a science base for this approach requires research in device design, modeling, and algorithms.

As a feasibility study, we perform experiments to characterize the dynamic and frictional properties of microscopic parts when placed on a vibrating substrate and in electrostatic fields. We first demonstrate that ultrasonic vibration can be used to overcome friction and adhesion of small parts. In a second set of experiments, we describe how parts are accurately positioned using electrostatic traps. We are also working to model part behavior as a first step toward the systematic design of planar force fields where the input is part geometry and desired final arrangement, and the output is an electrode pattern that produces the appropriate planar force field.

5.1 Experimental Apparatus

A piezoelectric actuator supports a vibratory table consisting of a rigid aluminum base, which has a flat glass plate ($25mm \times 25mm \times 2mm$) attached to its top. A thin chrome-gold layer ($1000\mathring{A}$) is evaporated onto the glass and patterned using photolithography. The signal from a function generator is amplified and transformed to supply the input voltage for the piezo transducer. The piezo is driven at ultrasonic frequencies in the $20kHz$ range. At resonance we observe amplitudes of up to $500nm$ (measured with laser interferometry), which correspond to accelerations of several hundred g's. Figure 12 shows a diagram of the experimental setup. The current experimental apparatus is shown in Figure 13. The apparatus can be operated in air or in a vacuum chamber.

Voltage is applied between the aluminum vibratory table and the chrome-gold electrode, which together act as a parallel plate capacitor. The applied voltage is limited by the breakdown voltage of air and glass and the path length (air: $3 \cdot 10^6 \frac{V}{m} \ 1cm = 30kV$; glass: $10^9 \frac{V}{m} \ 2mm = 2MV$). The patterned top electrode creates fringing electrostatic fields. Its
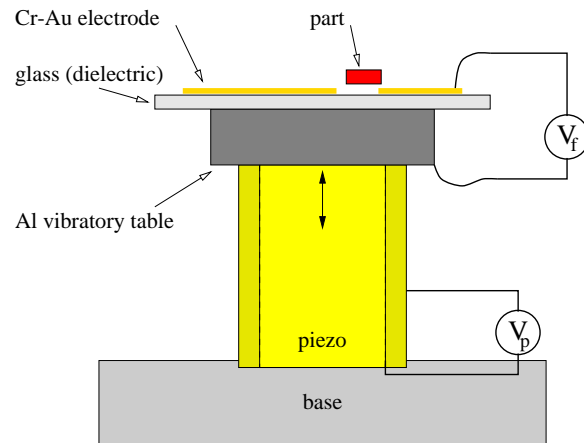
Figure 12: Experimental apparatus for self assembly with electrostatic traps. A vibratory table with a gold-covered dielectric is attached to a piezoelectric actuator. The aperture in the upper electrode creates a fringing field that causes polarization in the part. The part is attracted to the aperture. (Reprinted from [12]. © 1998 IEEE.)
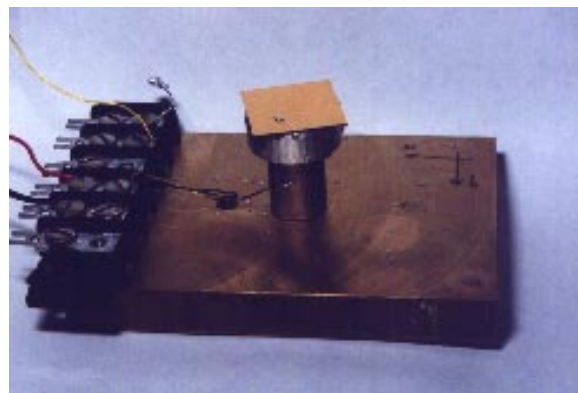

Figure 13: Experimental apparatus for self assembly experiments. A lithographically patterned electrode is attached to a piezoelectric actuator (vertical cylinder). Some parts can be seen in the lower left quadrant of the substrate. (Reprinted from [12]. © 1998 IEEE.)
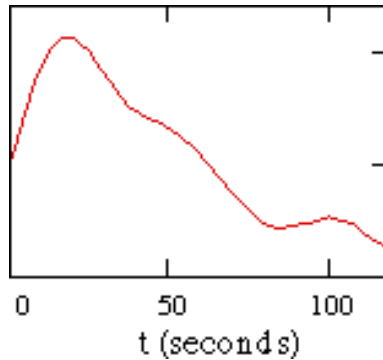
Figure 14: Histogram of binding times for electrostatic trapping, from an experiment with a total of 70 sample runs. Data exhibits an exponential distribution. (Reprinted from [12]. © 1998 IEEE.)

effect is a potential field whose minima lie at apertures in the top electrode. Parts are attracted to these electrostatic "traps."

The parts employed in our experiments are mainly surface-mount diodes and capacitors. They usually have rectangular shapes with dimensions between $0.75mm$ and $2mm$. We also performed experiments with short pieces of gold wire ($0.25mm$ diameter).

5.2   Experimental Observations

Overcoming Friction and Adhesion.   Small parts were randomly distributed on the substrate. When no signal is applied to the piezo, the parts tend to stick to the substrate and to each other, due to static charges, capillary or van der Waals forces. When applying sinusoidal signals of various frequencies and amplitude, the parts break contact. This behavior was particularly pronounced at resonance frequencies (e.g. observed in the $20kHz$ range). In this case the motion of the parts resembles liquid: tilting of the substrate surface by less than 0.2 percent was sufficient to influence their direction of (down-slope) motion. This implies a friction coefficient $\mu < 0.002$.

When the substrate surface was leveled carefully, the parts exhibited random Brownian motion patterns, until they settled in a regular grid pattern. This important observation is a strong indication that the system is sufficiently sensitive to react even to very small surface forces.

At high signal amplitudes, the vibration induces random bouncing of the parts. Reducing the amplitude accomplishes an annealing effect; at lower amplitudes only in-plane translations and rotation occurs. After such annealing sequences, surface mount diodes consistently settled with their solder bumps facing up. This observation suggests that even very small asymmetries in part design can be exploited to influence its final rest position. Voltages of $V_{pp} = 2V$ were sufficient to sustain free motion of the parts. This corresponds to a vibration amplitude of approximately $30nm$.

Vacuum Experiments. These experiments were repeated both in air and in low vacuum (high mTorr range). First results indicate that the energy required to overcome adhesive forces decreases with pressure, probably due to squeeze film effects [23], and due to the vacuum created between the flat part bottom surface and the substrate when operated at ultrasonic frequencies. As a result, the atmospheric pressure acting on the top surface presses the part onto the surface. For example, simple calculations show that if a rectangular part with dimensions $1mm \times 1mm \times 0.1mm$ and mass $0.1mg$ were exposed to atmospheric pressure on one side and to vacuum on the other side, it experienced an acceleration of nearly 100,000 g.

Electrostatic Self-Assembly and Sorting. The electrode design represents a parallel-plate capacitor with apertures in the upper electrode. The resulting fringing fields induce polarization in neutral parts, so that they are attracted to the apertures, and get trapped there. Once a part is trapped, it reduces the fringing field, which prevents attraction of more parts to this location. Figure 16 shows the positioning of four surface mount capacitors on four sites. The binding times for parts were automatically measured with an optical sensor and a recording oscilloscope. They exhibit an exponential distribution (Figure 14) with expected time of approximately 30 seconds.

Parts Sorting by Size. Large and small parts were mixed and placed randomly on a vibrating surface slightly tilted by $\approx 1°$. Vibration caused a sorting effect such that parts were separated with smaller parts settling at the lower end of the vibrating surface.

5.3 Modeling and Simulation

A variety of effects influence the behavior of the parts used in our microassembly experiments, among others (1) electrostatic fields created by capacitor plates, (2) conductivity or dielectric constants of parts, (3) induced dipoles, and (4) static charges on nonconductive and electrically isolated conductive parts.

Results from modeling based on a smooth approximation of the electrostatic potential are shown in Figure 15. The potential U is created by an electrode design as shown in Figure 16. The corresponding planar force field $F = \nabla U$ is shown in Figure 15(b), together with a simulation of a part moving in the field. In this simulation, the effective force on the part F_P was determined by integrating the force field over the part area $F_P = \int_P F \; dA$ (a more accurate model will take into account the deformation of the field by the part, as well as e.g. changes in its induced charge distribution). Then the force F_P is integrated over time to determine the part motion.

5.4 Algorithmic Issues for Massively Parallel Manipulation

As shown in the previous sections, planar force fields (PFFs) constitute a useful tool to model massively-parallel, distributed manipulation based on geometric and physical reasoning. Applications such as parts-feeding can be formulated in terms of the force fields required. Hence, planar force fields act as an abstraction between applications requiring parallel manipulation,
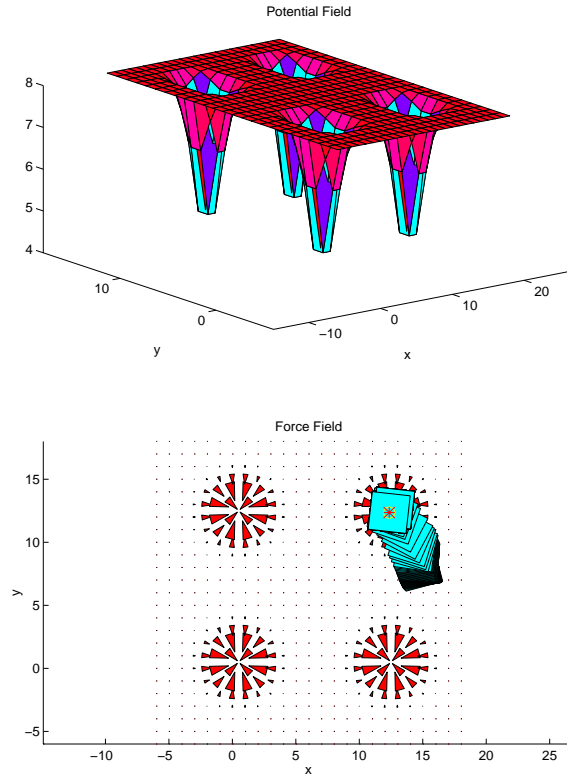
Figure 15: (a) Potential field created by an electrode with four small square-shaped apertures, as shown in the experimental setup in Figure 16. The four potential traps correspond to the four apertures. (b) Simulation of a square part moving in the corresponding force field (denoted by force vectors) The part translates and rotates until it reaches a local minimum in the potential field. (Reprinted from [12]. © 1998 IEEE.)

and their implementation e.g. with MEMS or vibratory devices. Such abstractions permit hierarchical design, and allow application designs with greater independence from underlying device technology.

Recently Developed PFFs.   In [10] Böhringer et al. established the foundations of massively parallel manipulation with force fields. Among the PFFs developed in the past years the following have been thoroughly investigated:

Squeeze Field: Squeeze fields are fields with unit forces pointing perpendicularly towards a straight *squeeze line* (e.g. $\vec{F}(x, y) = (-\text{sign}(x), 0)$). When placed in a squeeze field, every part reaches one out of a small number of possible equilibria.

Radial Field: A unit radial field is given by $\vec{F}(x, y) = -\frac{1}{\sqrt{(x^2 + y^2)}}(x, y)$ if $(x, y) \neq 0$, and 0 otherwise. In a radial field, any polygonal part has a unique *pivot point*. The part is

in a unique translational equilibrium if and only if its pivot point coincides with the center of the squeeze field.

Elliptic Field: The elliptic PFF (see Kavraki [37]) is a continuous field of the form $\vec{F}(x, y) = (-\alpha x, -\beta y)$, where α and β are two distinct positive constants. The field poses and orients non-symmetric parts into two stable equilibrium configurations.

Motion Planning with Artificial and Physical Potential Fields. Robotics motion planning is concerned with the problem of moving an object from an initial configuration q_i to a goal configuration q_g. In our case, a manipulation plan consists of a sequence of planar force fields. A general question that arises in the context of PFFs is the following: *Which force fields are suitable for manipulation strategies?* That is: can we characterize all those force fields in which every part has stable equilibria? To answer these questions, we use recent results from the theory of *potential fields.* It can be shown that certain PFFs that implement potential fields have this property, whereas fields without potential do not induce stable equilibria on all parts. Previous work has developed control strategies with *artificial* potential fields [40, 42, 63, 60], and discrete approximations to physical potential fields [11, 10]. The fields employed in this paper are non-artificial (*i.e., physical*). Artificial potential fields require a tight feedback loop, in which, at each clock tick, the robot senses its state and looks up a control (*i.e.,* a vector) using a state-indexed navigation function (*i.e.,* a vector field). In contrast, physical potential fields employ no sensing, and the motion of the manipulated object evolves open-loop (for example, like a body in a gravity field). Hence, for physical potential fields such as electrostatic fields, the motion planning problem has to be solved during device design. A design algorithm takes as input part geometry and desired goal configurations, and returns an electrode geometry that creates the proper potential field. During execution, the systems runs open-loop. We believe that this shift of complexity from run-time to design-time is crucial for efficient parallel microassembly methods.

5.5   Summary

Our experiments show that friction and adhesion between small parts can be overcome by ultrasonic vibration. In such an effectively frictionless environment, we demonstrate that small parts can be accurately positioned in parallel with electrostatic traps. This research opens the door to parallelize the manufacture of a new generation of consumer and industrial products, such as hybrid IC / MEMS devices, flat panel displays, or VCSEL arrays.

The behavior of the parts on the substrate can be modeled using planar force fields, which describe the effective lateral force acting on the part (as a function of its location in configuration space). A key problem is to determine an electrode design that creates a specific planar force field, such that parts are reliably positioned and oriented at desired locations. We attack this problem by the development of efficient models for manipulation in electrostatic force fields, and with new algorithms for motion planning with planar force fields.

We believe that planar force fields have enormous potential for precise parallel assembly of small parts. The goal of this research is to develop an entirely new methodology for

precision part manipulation and to demonstrate it with new theory, algorithms, and high-performance devices. For updated information on this project see our WWW pages at www.ieor.berkeley.edu/~karl/MicroSelfAssembly.
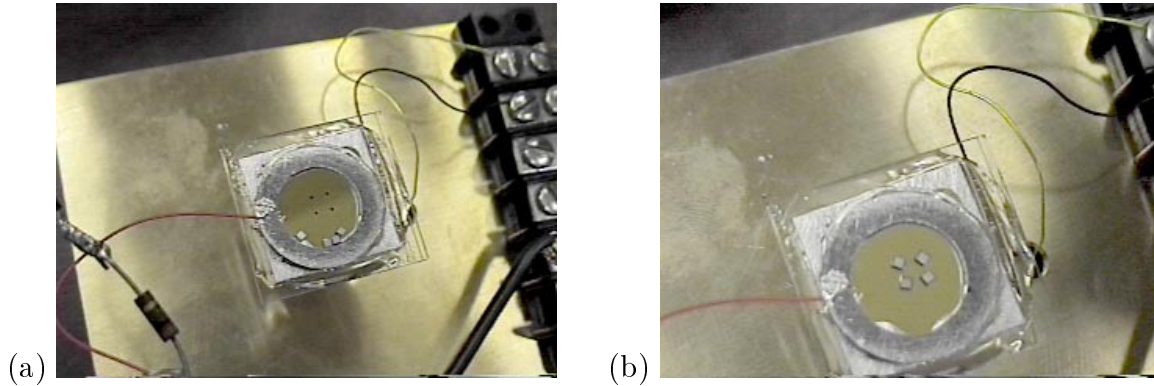

(a) (b)

Figure 16: Parallel microassembly with electrostatic force fields: (a) Surface-mount capacitors are placed onto a glass substrate with a $100nm$ thin patterned Cr-Au electrode. Frictional and adhesive forces are overcome by ultrasonic vibration. (b) Voltage applied to the electrode creates an electrostatic field. The parts are attracted to the apertures in the electrode (dark squares) and are trapped there. (Reprinted from [12]. © 1998 IEEE.)

6 Conclusion and Emerging Trends

Miroassembly is a challenging new area of research. This chapter constitutes an initial attempt to identify important issues in this field. We investigate surface sticking effects at the micro scale, give a taxonomy of microassembly techniques, discuss a hierarchy of assembly forces, and outline a brief summary of the current state of the art in microassembly. We also discuss a specific new technique for massively parallel assembly, by employing vibration to overcome adhesion and electrostatic forces to position micro parts in parallel.

Advances in the field of microassembly can be expected to have enormous impact on the development of future miniaturized consumer products such as *e.g.* data storage systems or wireless communication devices. Techniques known from robotics such as vibratory parts feeding, teleoperation, or sensorless and planar force field manipulation provide useful tools for research in microassembly. However, the possibly huge numbers of tiny parts employed in microassembly pose specific and unique challenges that will require innovative or unconventional solutions. These results may in turn inspire new approaches and techniques for macroscopic robots.

Acknowledgments

References

[1] R. L. Alley, G. J. Cuan, R. T. Howe, and K. Komvopoulos. The effect of release-etch processing on surface microstructure stiction. In *Proc. Solid State Sensor and Actuator Workshop*, pages 202–207, Hilton Head Island, SC, June 1992.

[2] R. L. Alley, P. Mai, K. Komvopoulos, and R. T. Howe. Surface roughness modification of interfacial contacts in polysilicon. In *Transducers — Digest Int. Conf. on Solid-State Sensors and Actuators*, pages 288–291, San Francisco, CA, June 1994.

[3] K. M. Anderson and J. E. Colgate. A model of the attachment/detachment cycle of electrostatic micro actuators. In *Proc. ASME Micromechanical Sensors, Actuators, and Systems*, volume DSC 32, pages 255–268, Atlanta, GA, Dec. 1991.

[4] Y. Ando, H. Ogawa, and Y. Ishikawa. Estimation of attractive force between approached surfaces. In *Second Int. Symp. on Micro Machine and Human Science*, pages 133–138, Nagoya, Japan, Oct. 1991.

[5] F. Arai and T. Fukuda. A new pick up and relase method by heating for micromanipulation. In *Proc. IEEE Workshop on Micro Electro Mechanical Systems (MEMS)*, Nagoya, Japan, 1997.

[6] A. A. Berlin and K. J. Gabriel. Distributed MEMS: New challenges for computation. *IEEE Computer Science and Engineering*, pages 17–29, January – March 1997.

[7] K.-F. Böhringer, V. Bhatt, B. R. Donald, and K. Y. Goldberg. Sensorless manipulation using transverse vibrations of a plate. *Algorithmica*, 1998. To appear in Special Issue on Algorithmic Foundations of Robotics.

[8] K.-F. Böhringer, V. Bhatt, and K. Y. Goldberg. Sensorless manipulation using transverse vibrations of a plate. In *Proc. IEEE Int. Conf. on Robotics and Automation (ICRA)*, pages 1989–1996, Nagoya, Japan, May 1995. .

[9] K.-F. Böhringer, M. B. Cohn, K. Goldberg, R. Howe, and A. Pisano. Electrostatic self-assembly aided by ultrasonic vibration. In *AVS 44th National Symposium*, San Jose, CA, Oct. 1997.

[10] K.-F. Böhringer, B. R. Donald, N. C. MacDonald, G. T. A. Kovacs, and J. W. Suh. Computational methods for design and control of MEMS micromanipulator arrays. *Computer Science and Engineering*, pages 17–29, January – March 1997.

[11] K.-F. Böhringer, B. R. Donald, R. Mihailovich, and N. C. MacDonald. A theory of manipulation and control for microfabricated actuator arrays. In *Proc. IEEE Workshop on Micro Electro Mechanical Systems (MEMS)*, pages 102–107, Oiso, Japan, Jan. 1994. .

[12] K.-F. Böhringer, K. Goldberg, M. B. Cohn, R. Howe, and A. Pisano. Parallel microassembly with electrostatic force fields. In *Proc. IEEE Int. Conf. on Robotics and Automation (ICRA)*, Leuven, Belgium, May 1998.

[13] G. Boothroyd, C. Poli, and L. E. Murch. *Automatic Assembly*. Marcel Dekker, Inc., 1982.

[14] R. A. Bowling. A theoretical review of particle adhesion. In K. L. Mittal, editor, *Particles on Surfaces 1: Detection, Adhesion and Removal*, pages 129–155. Plenum Press, New York, 1988.

[15] M. B. Cohn. Self-assembly of microfabricated devices. United States Patent 5 355 577, Sept. 1992.

[16] M. B. Cohn. *Assembly Techniques for Microelectromechanical Systems*. PhD thesis, University of California at Berkeley, Department of Electrical Engineering and Computer Sciences, 1998.

[17] M. B. Cohn and R. T. Howe. Wafer-to-wafer transfer of microstructures using break-away tethers. United States Patent Application, May 1997.

[18] M. B. Cohn, R. T. Howe, and A. P. Pisano. Self-assembly of microsystems using non-contact electrostatic traps. *ASME-IC*, 1995.

[19] M. B. Cohn, C. J. Kim, and A. P. Pisano. Self-assembling electrical networks as application of micromachining technology. In *Transducers — Digest Int. Conf. on Solid-State Sensors and Actuators*, San Francisco, CA, June 1991.

[20] M. B. Cohn, Y. Liang, R. T. Howe, and A. P. Pisano. Wafer-to-wafer transfer of microstructures for vacuum packaging. In *Proc. Solid State Sensor and Actuator Workshop*, Hilton Head, NC, June 1996.

[21] G. Danuser, I. Pappas, B. Vögeli, W. Zesch, and J. Dual. Manipulation of microscopic objects with nanometer precision: Potentials and limitations in nano-robot design. *Int. Journal of Robotics Research*, 1997. Submitted for review.

[22] M. A. Erdmann and M. T. Mason. An exploration of sensorless manipulation. *IEEE Journal of Robotics and Automation*, 4(4), Aug. 1988.

[23] R. S. Fearing. A planar milli-robot on an air bearing. In *International Symposium of Robotics Research (ISRR)*, Heitsching, Germany, Oct. 1995.

[24] R. S. Fearing. Survey of sticking effects for micro parts handling. In *IEEE/RSJ Int. Workshop on Intelligent Robots & Systems (IROS)*, Pittsburgh, PA, 1995.

[25] J. T. Feddema and R. W. Simon. CAD-driven microassembly and visual servoing. In *Proc. IEEE Int. Conf. on Robotics and Automation (ICRA)*, Leuven, Belgium, May 1998.

[26] H. Fujita. Group work of microactuators. In *International Advanced Robot Program Workshop on Micromachine Technologies and Systems*, pages 24–31, Tokyo, Japan, Oct. 1993.

[27] K. Y. Goldberg. Orienting polygonal parts without sensing. *Algorithmica*, 10(2/3/4):201–225, August/September/October 1993.

[28] S. Hara, H. Nakada, R. Sawada, and Y. Isomura. High precision bonding of semiconductor laser diodes. *Int. J. Japan Soc. Prec. Eng,*, 27(1):49–53, Mar. 1993.

[29] W. R. Harper. *Contact and Frictional Electrification*. Clarendon Press, Oxford, 1967.

[30] L. Hecht. An introductory review of particle adhesion to solid surfaces. *Journal of the IES*, 33(2):33–37, Mar. – Apr. 1990.

[31] H. Hitakawa. Advanced parts orientation system has wide application. *Assembly Automation*, 8(3), 1988.

[32] R. G. Horn and D. T. Smith. Contact electrification and adhesion between dissimilar materials. *Science*, 256(5055):362—364, Apr. 1992.

[33] K. Hosokawa, I. Shimoyama, and H. Miura. Dynamics of self-assembling systems — analogy with chemical kinetics. *Artificial Life*, 1(4), 1995.

[34] J. N. Israelachvili. The nature of Van der Waals forces. *Contemp. Physics*, 15(2):159–177, 1974.

[35] T. B. Jones. *Electromechanics of Particles*. Cambridge University Press, 1995.

[36] R. Kaneko. Microtribology related to MEMS. In *Proc. IEEE Workshop on Micro Electro Mechanical Systems (MEMS)*, pages 1–8, Nara, Japan, Jan. 30 – Feb. 2 1991.

[37] L. Kavraki. Part orientation with programmable vector fields: Two stable equilibria for most parts. In *Proc. IEEE Int. Conf. on Robotics and Automation (ICRA)*, Albuquerque, New Mexico, Apr. 1997.

[38] C. Keller and R. T. Howe. Nickel-filled hexsil thermally actuated tweezers. In *Transducers — Digest Int. Conf. on Solid-State Sensors and Actuators*, Stockholm, Sweden, June 1995.

[39] C. G. Keller and R. T. Howe. Hexsil tweezers for teleoperated micro-assembly. In *Proc. IEEE Workshop on Micro Electro Mechanical Systems (MEMS)*, pages 72–77, Nagoya, Japan, Jan. 1997.

[40] O. Khatib. Real time obstacle avoidance for manipulators and mobile robots. *Int. Journal of Robotics Research*, 5(1):90–99, Spring 1986.

[41] C.-J. Kim, A. P. Pisano, , and R. S. Muller. Silicon-processed overhanging microgripper. *Journal of Microelectromechanical Systems*, 1(1):31–36, Mar. 1992.

[42] D. E. Koditschek and E. Rimon. Robot navigation functions on manifolds with boundary. *Advances in Applied Mathematics*, 1988.

[43] H. Krupp. Particle adhesion theory and experiment. *Advances in Colloid and Interface Science*, 1:111–239, 1967.

[44] B. A. Kwetkus, B. Gellert, and K. Sattler. Discharge phenomena in contact electrification. In *Int. Phys. Conf. Series No. 118: section 4, Electrostatics*, pages 229–234, 1991.

[45] R. Legtenberg, H. A. C. Tilmans, J. Elders, and M. Elenspoek. Stiction of surface micromachined structures after rinsing and drying: model and investigation of adhesion mechanisms. *Sensors and Actuators*, 43:230–238, 1994.

[46] C. Liu, T. Tsao, P. Will, Y. Tai, and W. Liu. A micro-machined magnetic actuator array for micro-robotics assembly systems. In *Transducers — Digest Int. Conf. on Solid-State Sensors and Actuators*, Stockholm, Sweden, June 1995.

[47] W. Liu and P. Will. Parts manipulation on an intelligent motion surface. In *IEEE/RSJ Int. Workshop on Intelligent Robots & Systems (IROS)*, Pittsburgh, PA, 1995.

[48] J. Lowell. Contact electrification of silica and soda glass. *J. Phys. D: Appl. Phys.*, 23:1082–1091, 1990.

[49] J. Lowell and A. C. Rose-Innes. Contact electrification. *Advances in Physics*, 29(6):947–1023, 1980.

[50] J. E. Luntz and W. Messner. A distributed control system for flexible materials handling. *IEEE Control Systems*, 17(1), Feb. 1997.

[51] J. E. Luntz, W. Messner, and H. Choset. Parcel manipulation and dynamics with a distributed actuator array: The virtual vehicle. In *Proc. IEEE Int. Conf. on Robotics and Automation (ICRA)*, pages 1541–1546, Albuquerque, New Mexico, Apr. 1997.

[52] P. Moncevicz, M. Jakiela, and K. Ulrich. Orientation and insertion of randomly presented parts using vibratory agitation. In *ASME 3rd Conference on Flexible Assembly Systems*, September 1991.

[53] M. Morita, T. Ohmi, E. Hasegawa, M. Kawakami, and M. Ohwada. Growth of native oxide on a silicon surface. *J. Appl. Physics*, 68(3):1272–1281, 1990.

[54] M. Nakasuji and H. Shimizu. Low voltage and high speed operating electrostatic wafer chuck. *Journal of Vacuum Science & Technology A (Vacuum, Surfaces, and Films)*, 10(6):3573–8, Nov.–Dec. 1992.

[55] B. Nelson and B. Vikramaditya. Visually guided microassembly using optical microscopes and active vision techniques. In *Proc. IEEE Int. Conf. on Robotics and Automation (ICRA)*, Albuquerque, NM, Apr. 1997.

[56] K. S. J. Pister, R. Fearing, and R. Howe. A planar air levitated electrostatic actuator system. In *Proc. IEEE Workshop on Micro Electro Mechanical Systems (MEMS)*, pages 67–71, Napa Valley, California, Feb. 1990.

[57] K. S. J. Pister, M. W. Judy, S. R. Burgett, and R. S. Fearing. Microfabricated hinges. *Sensors and Actuators A*, 33(3):249–256, June 1992.

[58] K. L. Prime and G. M. Whitesides. Self-assembled organic monolayers are good model systems for studying adsorption of proteins at surfaces. *Science*, 252, 1991.

[59] A. E. Quaid and R. L. Hollis. Cooperative 2-dof robots for precision assembly. In *Proc. IEEE Int. Conf. on Robotics and Automation (ICRA)*, Minneapolis, MN, Apr. 1996.

[60] J. Reif and H. Wang. Social potential fields: A distributed behavioral control for autonoomous robots. In K. Goldberg, D. Halperin, J.-C. Latombe, and R. Wilson, editors, *International Workshop on Algorithmic Foundations of Robotics (WAFR)*, pages 431–459. A. K. Peters, Wellesley, MA, 1995.

[61] D. Reznik, J. F. Canny, and K. Y. Goldberg. Analysis of part motion on a longitudinally vibrating plate. In *IEEE/RSJ Int. Workshop on Intelligent Robots & Systems (IROS)*, Grenoble, France, Sept. 1997.

[62] F. J. Riley. *Assembly Automation, A Management Handbook*. Industrial Press, New York, 1983.

[63] E. Rimon and D. Koditschek. Exact robot navigation using artificial potential functions. *IEEE Transactions on Robotics and Automation*, 8(5), October 1992.

[64] B.-Z. Sandler. *Robotics: Designing the Mechanisms for Automated Machinery*. Prentice Hall, 1991.

[65] P. R. Scheeper, J. A. Voorthuyzen, W. Olthius, and P. Bergveld. Investigation of attractive forces between PECVD silicon nitride microstructures and an oxidized silicon substrate. *Sensors and Actuators A (Physical)*, 30:231–239, 1992.

[66] C. T. Seto and G. M. Whitesides. Self-assembly of a hydrogen-bonded 2+3 supramolecular complex. *J. Am. Chem. Soc.*, 113, 1991.

[67] I. Shimoyama. Scaling in microrobotics. In *IEEE/RSJ Int. Workshop on Intelligent Robots & Systems (IROS)*, Pittsburgh, PA, 1995.

[68] A. Singh, D. A. Horsley, M. B. Cohn, A. P. Pisano, and R. T. Howe. Batch transfer of microstructures using flip-chip solder bump bonding. In *Transducers — Digest Int. Conf. on Solid-State Sensors and Actuators*, Chicago, IL, June 1997.

[69] U. Srinivasan and R. Howe, 1997. Personal communication.

[70] C. W. Storment, D. A. Borkholder, V. Westerlind, J. W. Suh, N. I. Maluf, and G. T. A. Kovacs. Flexible, dry-released process for aluminum electrostatic actuators. *Journal of Microelectromechanical Systems*, 3(3):90–96, Sept. 94.

[71] J. W. Suh, S. F. Glander, R. B. Darling, C. W. Storment, and G. T. A. Kovacs. Combined organic thermal and electrostatic omnidirectional ciliary microactuator array for object positioning and inspection. In *Proc. Solid State Sensor and Actuator Workshop*, Hilton Head, NC, June 1996.

[72] S. M. Sze. *Physics of Semiconductor Devices*. Wiley, New York, 2nd edition, 1981.

[73] A. Torii, M. Sasaki, K. Hane, and S. Okuma. Adhesive force distribution on microstructures investigated by an atomic force microscope. *Sensors and Actuators A (Physical)*, 44(2):153–8, Aug. 1994.

[74] G. M. Whitesides, J. P. Mathias, and C. T. Seto. Molecular self-assembly and nanochemistry: A chemical strategy for the synthesis of nanostructures. *Science*, 254, 1991.

[75] H.-J. Yeh and J. S. Smith. Fluidic self-assembly for the integration of GaAs light-emitting diodes on Si substrates. *IEEE Photonics Technology Letters*, 6(6):706–708, June 1994.

[76] H.-J. Yeh and J. S. Smith. Fluidic self-assembly of microstructures and its application to the integration of GaAs on Si. In *Proc. IEEE Workshop on Micro Electro Mechanical Systems (MEMS)*, pages 279–284, Oiso, Japan, Jan. 1994.

[77] H.-J. Yeh and J. S. Smith. Integration of GaAs vertical cavity surface-emitting laser on Si by substrate removal. *Applied Physics Letters*, 64(12):1466–1468, 1994.

[78] W. Zesch. *Multi-Degree-of-Freedom Micropositioning Using Stepping Principles*. PhD thesis, Swiss Federal Institute of Technology, Zürich, Switzerland, 1997.

[79] A. D. Zimon. *Adhesion of dust and powder*. Plenum Press, New York, 1969.